Applied Clay Science 132–133 (2016) 343–352

Contents lists available at ScienceDirect

Applied Clay Science

journal homepage: www.elsevier.com/locate/clay

Research paper

Adsorption of phosphate by acid-modified fly ash and palygorskite in aqueous solution: Experimental and modeling

Feihu Li [a,*], Wenhao Wu [a], Renying Li [b], Xiaoru Fu [a]

[a] CICAEET Center, AEMPC Lab, School of Environmental Science and Engineering, Nanjing University of Information Science and Technology, Nanjing 210044, China
[b] Jiangsu Key Laboratory of Agricultural Meteorology, College of Applied Meteorology, Nanjing University of Information Science and Technology, Nanjing 210044, China

ARTICLE INFO

Article history:
Received 9 January 2016
Received in revised form 30 June 2016
Accepted 30 June 2016
Available online 7 July 2016

Keywords:
Phosphate
Fly ash
Palygorskite
Adsorption
Surface complexation modeling
Generalized composite approach

ABSTRACT

In this study, a class F fly ash and palygorskite have been acid-modified and then evaluated for the adsorption of phosphate in aqueous solution via bench-scale batch experiments. XRD, XRF, SEM, and FTIR were employed to characterize the acid-modified fly ash (MFA) and palygorskite (MPal). Both MFA and MPal show enhanced phosphate adsorption after the modification treatment. The effects of pH, adsorbent dosage, and co-ions on phosphate adsorption, as well as adsorption thermodynamics and kinetics, and leaching features of spent (used) adsorbents were also investigated. The isotherms data fit well with the Langmuir model rather than the Freundlich model, giving maximum capacities (298 K) of 13.3 mg P g^{-1} for MFA and 10.5 mg P g^{-1} for MPal, respectively. Surface complexation modeling of P adsorption data with the nonelectrostatic generalized composite (GC) approach indicates that phosphate were directly bound to the metal centers by ligand exchange to form two monodentate complexes, $\equiv SHPO_4^-$ and $\equiv SPO_4^{2-}$. The GC model appears to be an easy and efficient tool to provide an insight into the mechanism of phosphate adsorption on complex adsorbents with limited model parameters. Leaching test results suggest that the spent adsorbents can be safely disposed or further reused.

© 2016 Elsevier B.V. All rights reserved.

1. Introduction

Phosphorus (P) is an essential nutrient to the growth of aquatic algal and other biological organisms; however, the excessive presence of phosphate in natural water bodies, especially lakes or reservoirs, will lead to algal blooms and eventually results in degeneration of water quality. This process is well known as eutrophication (Correll, 1998). Eutrophication of the Taihu Lake (Jiangsu, China) in the summer of 2007 caused a serious water crisis to both domestic and industrial users. Removal of phosphate, using either chemical or biological technologies, from such water bodies and inflows can therefore be effective to control the eutrophication of the lakes. Phosphate can be removed from wastewater by adsorption, ion-exchange, precipitation, biological uptake, etc. (Mayer et al., 2013). Of these approaches of phosphate removal, adsorption has attracted more attention due to its simplicity, stability, and operability (Agyei et al., 2000; Das et al., 2006; Yan et al., 2007; Haghseresht et al., 2009; Zamparas et al., 2012). The adsorption of phosphate by commercial adsorbents, industrial by-products, and clay minerals has been practiced for decades. Industrial by-products (e.g., fly ash) and natural clays (e.g., palygorskite, bentonite) are getting more attractive in phosphate removal other than commercial adsorbents due to their lower cost, abundance, and excellent adsorption capabilities (Ye et al., 2006; Yan et al., 2007; Gan et al., 2009; Haghseresht et al., 2009; Zamparas et al., 2012). In fact, there are a variety of fly ash sources (e.g., coal-fired power plants) as well as clay mines (e.g., palygorskite mines) around the Taihu lake. It would be promising to solve the eutrophication problem of the Taihu lake if the abundant and cheap fly ash and/or palygorskite can be utilized as adsorbents for phosphorous removal from municipal sewages that used to be discharged into the lake without any treatments.

Fly ash is a by-product derived from the combustion of pulverized coal in power plants. The utilization of fly ash for phosphate removal from wastewaters has been studied extensively recently, and the results have indicated that fly ash is an excellent alternative adsorbent to commercial adsorbents in phosphate adsorption (Ugurlu and Salman, 1998; Agyei et al., 2000, 2002; Grubb et al., 2000; Chen et al., 2007; Lu et al., 2009; Xu et al., 2010). It is reported that most of dissolved phosphate can be efficiently precipitated by the high concentration of calcium in class C fly ash (i.e., one type of fly ash generally contains >20% CaO) (Ugurlu and Salman, 1998; Lu et al., 2009). For class F fly ash (i.e., one type of fly ash contains <7% CaO), metal oxides in fly ash, such as Al_2O_3, Fe_2O_3, etc., can also uptake phosphate efficiently (Grubb et al., 2000; Chen et al., 2007). The phosphate adsorption capacity of class C fly ash is generally greater than that of class F fly ash due to the additional contribution from precipitation by the high content of calcium in Class C fly ash besides the adsorption of phosphate by metal oxides in both types of fly ashes (Agyei

* Corresponding author.
E-mail address: favorlee@163.com (F. Li).

http://dx.doi.org/10.1016/j.clay.2016.06.028
0169-1317/© 2016 Elsevier B.V. All rights reserved.

et al., 2000; Grubb et al., 2000; Chen et al., 2007; Yan et al., 2007). On the other hand, palygorskite (Pal, $(Mg,Al)_5(Si,Al)_8O_{20}(OH)_2 \cdot 8H_2O$) is a naturally occurring layered aluminum silicate mineral, which was widely used in catalyst, catalyst supports (Zhang et al., 2010, 2014; Pushpaletha and Lalithambika, 2011), and adsorbents (Ye et al., 2006; Gan et al., 2009). Previous studies have confirmed that phosphate can be effectively removed by both natural and modified palygorskites (Ye et al., 2006; Gan et al., 2009).

To obtain a higher adsorption capacity, some surface modifications (e.g., introducing or incorporating new groups, thermal treatment, acid activation, etc.) to these adsorbents are required. Haghseresht et al. (2009) found that incorporating lanthanum into bentonite can improve its adsorption capacity for phosphate in aqueous solution. Similarly, a recent study by Zamparas et al. (2012) also showed that iron-modified bentonite can uptake more phosphate than unmodified bentonite. Indeed, the other two typical modification methods, i.e., thermal treatment and acid activation have long been used to produce sorbents for certain practical applications (Bergaya et al., 2006). It is suggested that thermal treatment of palygorskite can increase its adsorption capacity for phosphate (Gan et al., 2009). Ye et al. (2006) also investigated the effects of either thermal treatment or acid activation of palygorskite on phosphate adsorption, and suggested that both modification approaches can improve phosphate adsorption efficiently. Research by Li et al. (2006b) using class F fly ashes (FA) as adsorbent for phosphate had elucidated that both thermal treatment and acid activation can significantly enhance its adsorption capacity. It was also reported that both class F and class C fly ashes modified with sulfuric acid possess a higher phosphate adsorption capacity as compared to the original fly ashes due to the dissolution of the amorphous siliceous spherical particulates that embedded active components for phosphorous adsorption (Liang et al., 2010; Xu et al., 2010).

To gain an insight into the adsorption mechanism of phosphate onto mono-component adsorbent, surface complexation modeling is generally employed to quantitatively description of phosphate adsorption data (Goldberg and Sposito, 1985; Bleam et al., 1991; Nilsson et al., 1996; He et al., 1997; Gao and Mucci, 2001; Rahnemaie et al., 2007). For multi-component or complex adsorbents, however, it still remains a great challenge to use surface complexation modeling to explore the adsorption mechanism due to the complication, even though only a few attempts using constant capacitance model (CCM) (Grubb et al., 2000) and chemical equilibrium model (Johansson and Gustafsson, 2000) has been made. To date, the only successful example of modeling the adsorption data of complex adsorbents is the generalized composite (GC) modeling approach, which was developed by Davis et al. (1998), and can successfully describe and predict the adsorption behaviors of many radionuclide and rare earth ions onto soils (Davis et al., 2004; Tertre et al., 2008). However, GC modeling approach had not been used to fit and predict phosphate adsorption on complex adsorbents yet. To the best of our knowledge, this is the first work that shows how to use the powerful GC modeling approach to describe P adsorption over complex adsorbents, gaining insights into the mechanism of phosphate adsorption.

The objective of this study was twofold: first, to examine the feasibility of using acid-modified fly ash and palygorskite (termed as MFA and MPal) as adsorbents for phosphate uptake in aqueous solution via batch experiments, and second, to gain an insight into the adsorption mechanism of both acid-modified adsorbents via the GC surface complexation modeling. The influences of pH, co-ions, and adsorbent dosage on phosphate adsorption have been studied. Equilibrium and kinetics studies were also performed and fitted with related isotherm models (i.e., Langmuir and Freundlich models) and a kinetic model (i.e., the pseudo second-order rate model). Leaching tests were also conducted to evaluate the safety of disposal or further reuse of the spent (used) adsorbents.

2. Materials and methods

2.1. Materials

Class F fly ash (FA) was obtained from the electrostatic precipitator (ESP) ash-hopper III of No. 4 pulverized coal (lignite bituminous coal) boiler at Huaneng Changxing power plant (located in the southwest lakeshore of the Taihu lake), while the palygorskite (Pal) was originated from Xuyi County (Jiangsu, China). The chemical components of both FA and Pal were measured by X-ray fluorescence spectroscopy (XRF), and the results are listed in Table 1. All other chemicals (analytic reagent (A.R.) grade) were purchased from Sinopharm Chemical Reagent Co. Ltd. (Shanghai, China) and used as received. Milli-Q ultrapure water (18.2 MΩ·cm resistivity at 298 K) was used in all experiments.

2.2. Modification procedure

Three types of acid solution (Ye et al., 2006; Liang et al., 2010), including H_2SO_4 (2 mol L^{-1}), HCl (2 mol L^{-1}), and H_2SO_4–HCl mixture (1 mol L^{-1} H_2SO_4 + 1 mol L^{-1} HCl), were used to etch the original materials, i.e., fly ash and palygorskite. Typically, 20 g of FA or Pal was ground to pass through a 160 mesh-sized sieve (size <94 μm), followed by drying in 393 K (120 °C) oven and then well mixing with 100 mL of etching solution (e.g., 1 mol L^{-1} H_2SO_4 + 1 mol L^{-1} HCl) for 30 min under ultrasonication. The mixtures were then filtered and washed with excess water to provide salt-free sediments, followed by drying in oven (393 K), cooling to ambient temperature, and regrinding. Finally, the modified FA and Pal (termed as MFA and MPal, respectively) were resieved to pass through a 160 mesh-sized sieve prior to collecting and storing for further tests.

2.3. Characterization

X-ray diffraction (XRD) measurement was performed on an ARL X'TRA diffractometer (ARL, Switzerland) at a voltage of 40 kV and a current of 30 mA with Cu-Kα radiation. XRF data were collected on an ARL–9800 spectrometer following the fused–disc method (Li et al., 2006a). Scanning electron microscopy (SEM) was conducted on an S-3400 N microscope (Hitachi, Japan) with an accelerating voltage of 20 kV. Fourier transform infrared (FTIR) spectra were recorded on a NIKOLET Nexus 870 spectrometer (Thermo Fisher, USA) following the KBr–pressed–disc method (Li, 2013).

2.4. Phosphate adsorption tests

Phosphorous stock solutions (1000 mg L^{-1}) were prepared using A.R. grade K_2HPO_4. The effect of adsorbent dosage on phosphate adsorption was evaluated first, and the results (see Fig. S1 in the *supplementary data*) indicated that a dosage of 2 g L^{-1} of adsorbents is the optimum value in consideration of efficiency and costing. The pH effect experiments were performed to determine the adsorption envelope, which is the percentage of phosphorous adsorbed as a function of the solution pH. Dispersions containing 10 mg P L^{-1} (0.3226 mM) phosphate and 2 g L^{-1} adsorbents were adjusted to a desired pH in the range of 3–12 by using 0.1 M NaOH and HCl solution. After shaking on a rotary shaker at 200 rpm for at least 24 h to obtain equilibrium states, the suspensions were filtered with 0.45 μm cellulose membrane for P concentration measurement. Typical ions including F^-, SO_4^{2-}, CO_3^{2-}, Zn^{2+}, Cu^{2+}, and Al^{3+} (using NaF, Na_2SO_4, $Na_2CO_3 \cdot H_2O$, $Zn(NO_3)_2 \cdot 6H_2O$, $Cu(NO_3)_2$, and $Al(NO_3)_3$ as source salts, respectively) with concentrations of 5–40 mg L^{-1} were also selected to investigate the effect of co-ions on phosphate adsorption with a dosage of 2 g L^{-1} at pH 7.5 ± 0.1.

Adsorption kinetics experiments were carried out by reacting 10 mg P L^{-1} of phosphate with 2 g L^{-1} adsorbents at pH 7.5 ± 0.1. The kinetic data were fitted with the pseudo second-order rate model (Ho and

Table 1
Chemical composition of fly ash and palygorskite in terms of oxide contents. (wt.%).

Sample	SiO_2	Al_2O_3	Fe_2O_3	CaO	MgO	K_2O	Na_2O	TiO_2	P_2O_5	SO_3	LOI[a]
FA	45.29	41.35	3.57	3.21	0.63	0.62	N/A[b]	1.73	0.62	0.21	2.44
Pal	52.95	9.52	4.78	0.37	10.01	0.90	0.02	0.39	0.01	0.01	N/A

[a] LOI: loss on ignition at 960 °C.
[b] N/A: not available.

McKay, 1998) as given in Eqs. (1) and (2):

$$\frac{t}{q_t} = \frac{1}{v_0} + \frac{1}{q_e} t \tag{1}$$

$$v_0 = k_2 {q_e}^2 \tag{2}$$

where v_0 (mg $g^{-1}\cdot min^{-1}$) is the initial adsorption rate, q_e (mg g^{-1}) is the adsorption capacity at equilibrium, q_t (mg g^{-1}) is the adsorption capacity at time t, and t is contacting time (min), k_2 (g $mg^{-1}\cdot min^{-1}$) is the pseudo-second-order rate constant.

Adsorption isotherm experiments were conducted with the increasing P concentration (5–30 mg L^{-1}) in conical flasks. After adjusting pHs of these suspensions to 7.5 ± 0.1, these flasks were sealed and shaken at 200 rpm under controlled temperatures (i.e., 283 K, 298 K, and 313 K) for 24 h. Then, the mixtures were filtered for P analyses. The Langmuir and Freundlich equations (Eqs. (3) and (4)) were employed to fit the adsorption equilibrium data:

$$q_e = \frac{b q_m C_e}{1 + q_m C_e} \tag{3}$$

$$q_e = K_F {C_e}^{1/n} \tag{4}$$

where q_e is the equilibrium P adsorption capacity in mmol g^{-1}, C_e is the equilibrium P concentration in mmol L^{-1}, q_m is the maximum adsorption capacity in mmol g^{-1}, and b (L $mmol^{-1}$) is Langmuir adsorption energy constant. Both K_F and n are Freundlich constants.

Phosphorous concentration was determined by an UV–vis spectrophotometer (UV-9200, Beijing Rayleigh Instrument Co., China) at 700 nm following the ascorbic acid method (APHA, 1998).

2.5. Thermodynamic analysis

The thermodynamic parameters including standard free energy change (ΔG^0) and standard enthalpy change (ΔH^0) for the adsorption reaction are estimated by the following equations (Gibbs, 1873):

$$\Delta G^0 = -RTlnb \tag{5}$$

$$\Delta G^0 = \Delta H^0 - T\Delta S^0 \tag{6}$$

where ΔG^0 is the change of standard free energy in kcal mol^{-1}, ΔH^0 is the change of standard enthalpy in kcal mol^{-1}, ΔS^0 is the change of standard entropy in kcal mol^{-1} K^{-1}, T is the absolute temperature (K), R is the gas constant (i.e., 1.986 cal mol^{-1} K^{-1}), and b is the equilibrium constant from the Langmuir model.

The standard differential heat of adsorption can be determined from the Van't Hoff expression (Atkins and De Paula, 2006),

$$\ln b = -\frac{\Delta H^0}{RT} + constant \tag{7}$$

A plot of ln$b$ versus $1/T$ can yield a straight line, and ΔH^0 can be obtained from the slope of the line.

2.6. Surface complexation modeling

A generalized composite (GC) approach for surface complexation modeling without the electrostatic correction terms was employed to fit phosphate adsorption data using the speciation calculation software visual MINTEQ 3.1 (Gustafsson, 2014). In the GC approach, genetic surface sites are assumed to represent the whole mineral assemblage. This semi-empirical approach would reduce the complexity of modeling and can be used to simulate a number of adsorption processes over a range of solution conditions (Davis et al., 1998). Besides, the nonelectrostatic model does not require specifying the surface acidity reactions as well as the capacitance values of the electric double layer, further simplifying the modeling processes (Davis et al., 2004). Surface complexation reactions and SCM parameters given in Table S1 (see *Supplementary Data*) were either obtained from literature or optimized to best fit the experimental data by using the PEST package in combination with visual MINTEQ.

2.7. Leaching test of toxic ions

The leaching test of spent adsorbents was conducted following the *Solid waste–Extraction procedure for leaching toxicity–Horizontal vibration method* (HJ 557–2010) Phosphate leaching tests were also performed using the same method with different solid/water mass ratios (see Fig. S2). The concentrations of leachable toxic metal ions were measured on a J-A1100 inductively coupled plasma-atomic emission spectrometer (ICP-AES, Jarrell-Ash, USA).

3. Results and discussion

3.1. Characterizations of fly ash and palygorskite

Table 1 presents the chemical composition of FA and Pal as determined by X-ray fluorescence spectrometer (XRF). The XRF data suggest that the main elementary components of FA are silica, aluminum, iron, and calcium, whereas the elementary chemistry of Pal is dominated by silica, magnesium, aluminum, and iron. Moreover, it is noted that both the calcium content (3.21 wt.%) of FA and the residual carbon content (2.44 wt.%) as determined by the loss on ignition (LOI) test are low, which implies that the contribution of phosphate retention from either precipitation by soluble calcium ion or adsorption by residual carbon should be very tiny and hence ignored (Grubb et al., 2000).

XRD results (Fig. 1) indicate that FA mainly consists of mullite (JCPDS PDF # 15–0776) and an amorphous phase (see the diffuse scattering halo in 20–30° 2θ range of Fig. 1a), while the major minerals in Pal includes palygorskite (JSPDS PDF# 21-0958) and quartz (JSPDS PDF# 65-0466). In addition, the absence of hematite or lime reflections in the XRD pattern (Fig. 1a) suggests both iron and calcium are occurred in amorphous forms. After etching with acidic solution (i.e., 1 mol L^{-1} HCl + 1 mol L^{-1} H_2SO_4), most of the amorphous phase in FA dissolved accordingly (as verified by the disappearance of the diffuse scattering halo in Fig. 1b) and a new minor phase, gypsum (JSPDS PDF# 47–0964), grown as a result of the reaction between sulfuric acid and the soluble calcium ions. Likewise, it also shows that palygorskite can partly be dissolved upon the etching treatment, leading to a slight decrease of the reflection intensity (cf. Fig. 1c and d).

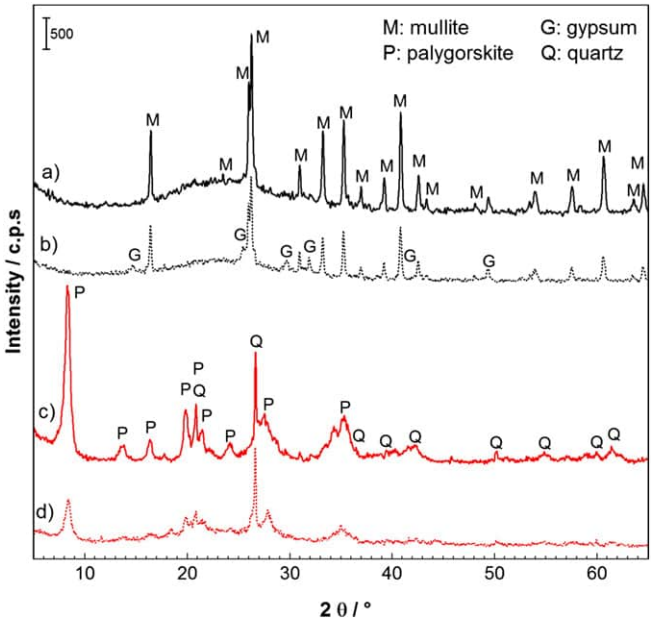

Fig. 1. XRD patterns of (a) fly ash, (b) modified fly ash (MFA), (c) palygorskite, and (d) modified palygorskite (MPal).

The morphological characteristic of both FA and Pal was examined with scanning electron microscopy (SEM). It is suggested that, from the SEM images (Fig. 2), FA was composed of spherical particles ranging from 1 to 10 μm, and Pal comprised of fibrous rods or bundles, forming

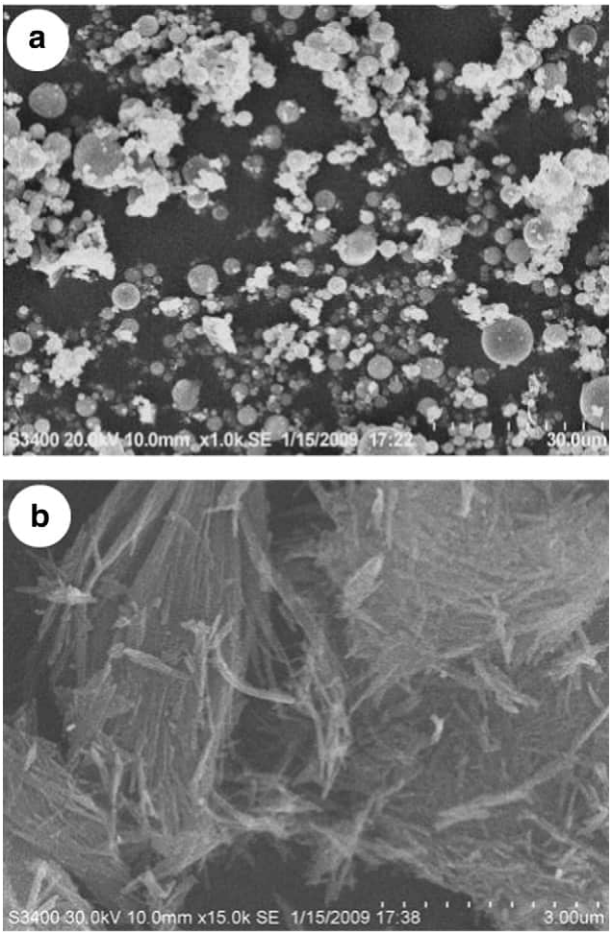

Fig. 2. SEM images of (a) fly ash and (b) palygorskite.

randomly oriented, highly packed scaffolds as described elsewhere (Gan et al., 2009).

Fig. 3 depicts the FTIR spectra of both FA and Pal before and after acid modification. The broad bond at 3650–3200 was attributed to adsorbed water molecular, and the band intensity increased after acid etching (Frost et al., 2001). The bands at 1622 cm^{-1}, 1637 cm^{-1}, 1660 cm^{-1}, and 1655 cm^{-1} were derived from the bending vibration of adsorbed water molecular (Frost et al., 2001; Wang et al., 2008). The bands at 1170 cm^{-1} in FA samples were attributed to antisymmetric Si-O-Si stretching vibration of SiO_4 tetrahedron while bands at 1104 cm^{-1} were assignable to antisymmetric stretching vibration of Si-O-Al network (Padmaja et al., 2001). The remaining weak bands in 900–400 cm^{-1} region were arose from stretching vibration of Al-O-Al except that at 464 cm^{-1} was from the bending vibration of O-Si-O in SiO_4 tetrahedron. The weak shoulder band centered at 537 cm^{-1} in the MFA spectrum (Fig. 3b) can be assignable to Fe—O stretching vibration of residual amorphous iron oxides (Frost et al., 2001; Padmaja et al., 2001). For Pal samples, the bands both around 1200 cm^{-1} and in the range of 1200–900 cm^{-1} were from the stretching vibration of Si—O bond. The band at 978 cm^{-1} along with the shoulder band at 880 cm^{-1} were due to the Si-O-H deformation vibration and the band at 481 cm^{-1} was attributed to the bending vibration of O-Si-O (Frost et al., 2001; Wang et al., 2008).

It should be noted that both the band intensity of absorbed water molecular and stretching vibration of Si-O-Si/Si-O-Al increased after the acid etching, suggesting that acid-etching treatment can efficiently dissolve the amorphous siliceous spherical particulates that embedded active components for phosphorous adsorption (Liang et al., 2010), and produce new surface –OH groups that probably account for the enhanced phosphate adsorption. In fact, surface hydroxyls including the aluminol group (≡AlOH) (Kasama et al., 2004) and ferrinol group (≡FeOH) (Wang et al., 2013), both of which are verified by the FTIR spectra, are among the most active sites for phosphate retention in aqueous solution.

3.2. Effect of acid modification methods

Fig. 4 illustrates the effect of acid modification with different acid solutions on the P adsorption with an initial phosphate concentration of 10 mg P L^{-1} and a dosage of 3 g L^{-1}. It is obvious that, under the

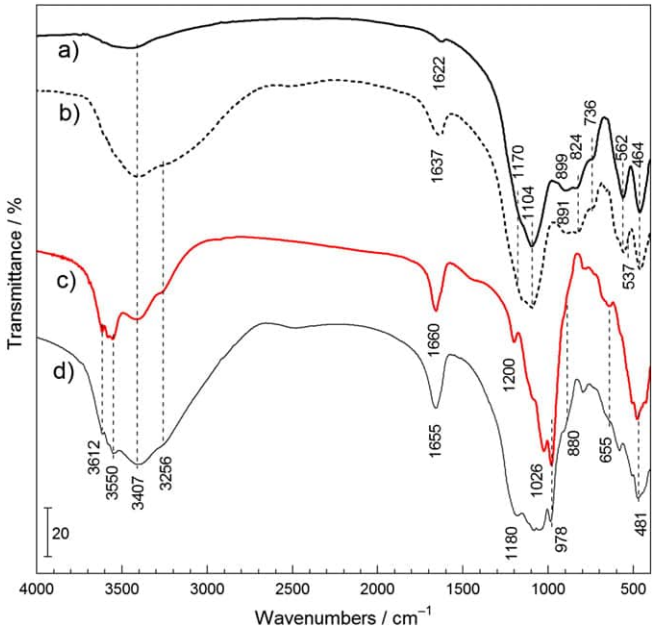

Fig. 3. FTIR spectra of (a) fly ash, (b) MFA, (c) palygorskite, and (d) MPal.

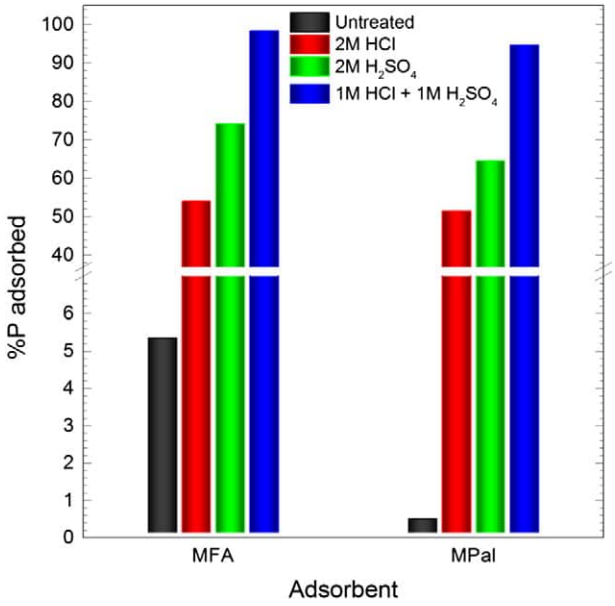

Fig. 4. Phosphate adsorption as a function of modifications of adsorbents ($[PO_4^{3-}]_{initial}$ = 10 mg P L^{-1}; dosage 3 g L^{-1}; pH 5.3 ± 0.1).

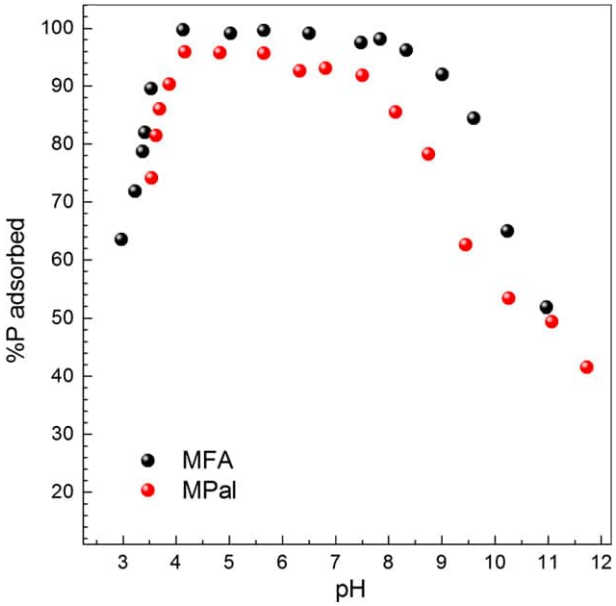

Fig. 5. Phosphate adsorption as a function of solution pH.

same conditions, the adsorbents modified with H_2SO_4–HCl mixture adsorbed more P other than adsorbents treated with 2 M HCl and 2 M H_2SO_4, over 94% and 98% of P being adsorbed by the H_2SO_4–HCl treated MPal and MFA, respectively. However, only 0.4% and 2.59% of P were fixed by untreated Pal and FA, respectively. The P adsorption capacities of MFA and MPal were 17 and 188 times higher than those of the untreated counterparts, respectively. The enhancement of P adsorption by both HCl- and H_2SO_4-treated MFA and MPal is also apparent, giving an improved capacity of at least 9–128 times higher than those of untreated samples. Accordingly, the H_2SO_4–HCl mixture was used as the etching solution for modification of FA and Pal due to its high performance in enhancing P adsorption. This high performance has also been confirmed by results of the effect dosage on phosphate adsorption (see Fig. S1).

3.3. Effect of pH

In general, the solution pH not only affects the speciation of phosphate anions, but also impacts the protonation/dissociation process of the surface hydroxyl and hence influences the adsorption behaviors of phosphate. For 10 mg P L^{-1} (0.3226 mM) phosphate solution at 298 K, the major species are H_3PO_4, $H_2PO_4^-$, and HPO_4^{2-}, respectively, for pH < 2.15, 2.15 < pH < 7.2 and 7.2 < pH < 12.3, according to the calculation results with visual MINTEQ (see Fig. S3). Moreover, it is expected that the surface site groups of both MFA and MPal are likely to be protonated in the acidic pH range, while their protons will dissociate from the hydroxyls in the alkaline pH range (Huertas et al., 1998). The results of pH influence on phosphate adsorption by both MFA and MPal are given in Fig. 5. Phosphate adsorption by both MFA and MPal shows a similar trend that uptake of phosphate increased with increasing pH from 3 to ~5, maintained stable for a certain range of pH, and then declined as pH increased from 7 to 12. This observation is in agreement with other reports showing that phosphate adsorption is more efficiently in acidic pH range other than alkaline pH range (Ye et al., 2006; Gan et al., 2009; Xue et al., 2009).

3.4. Effect of co-ions

Typical ions such as F^-, SO_4^{2-}, CO_3^{2-}, Zn^{2+}, Cu^{2+}, and Al^{3+} normally occurred with phosphate in either natural or waste waters. The effect of these co-ions on phosphate adsorption was studied with initial phosphate concentration of 10 mg P L^{-1}. The results illustrated in Fig. 6 reveal that bi- and trivalent cations, including Zn^{2+}, Cu^{2+}, and Al^{3+}, can efficiently improve phosphate adsorption by both MFA and MPal. One reason for this observation may involve the formation of less soluble compounds by reactions between phosphate and these cations as reported previously (Grubb et al., 2000; Johansson and Gustafsson, 2000; Bournonville et al., 2004). Besides, it might also be contributed from a positive charged surface of both adsorbents that resulted from adhesion of the bi- and trivalent cations to the surfaces, which then shifts their point of zero charge (pH_{PZC}) values to more alkaline range and enhances the adsorption of phosphate (Wilkie and Hering, 1996).

It is also suggested that phosphate adsorption by MPal was moderately affected by fluoride, but not depressed by sulfate, and carbonate (Fig. 5c and d). However, phosphate adsorption by MFA was slightly interfered by fluoride, but not impacted by sulfate, and carbonate. This phenomenon has also been reported for phosphate adsorption on modified palygorskite (Ye et al., 2006) and furnace slag (Xue et al., 2009). The competing effect observation also indicates that the adsorption mechanism of phosphate by both adsorbents are likely to be ligand exchange as described as follows (Goldberg and Sposito, 1984),

$$\equiv SOH + H_3PO_4 \leftrightarrow \equiv SH_2PO_4 + H_2O \quad (8)$$

$$\equiv SOH + H_2PO_4^- \leftrightarrow \equiv SHPO_4^- + H_2O \quad (9)$$

$$\equiv SOH + HPO_4^{2-} \leftrightarrow \equiv SPO_4^{2-} + H_2O \quad (10)$$

3.5. Adsorption kinetics

The adsorption kinetic curves of phosphate by both MFA and MPal are depicted in Fig. 7. The adsorption kinetic processes can be apparently divided into two stages: an initial rapid adsorption step in which over 90% of phosphate was adsorbed in the first 10 min and a slow adsorption step which lasted ~60 min to reach an equilibrium state (see Fig. 7a and inset). The two-stage adsorption kinetic processes have also been observed for phosphate adsorption by other adsorbents (Ye et al., 2006; Gan et al., 2009).

Besides, the adsorption kinetic data can be well-fit by the pseudo-second-order rate model (Fig. 7) as indicated by the high correlation coefficients, $R^2 > 0.99$ (Table 2). The model has been extensively used for

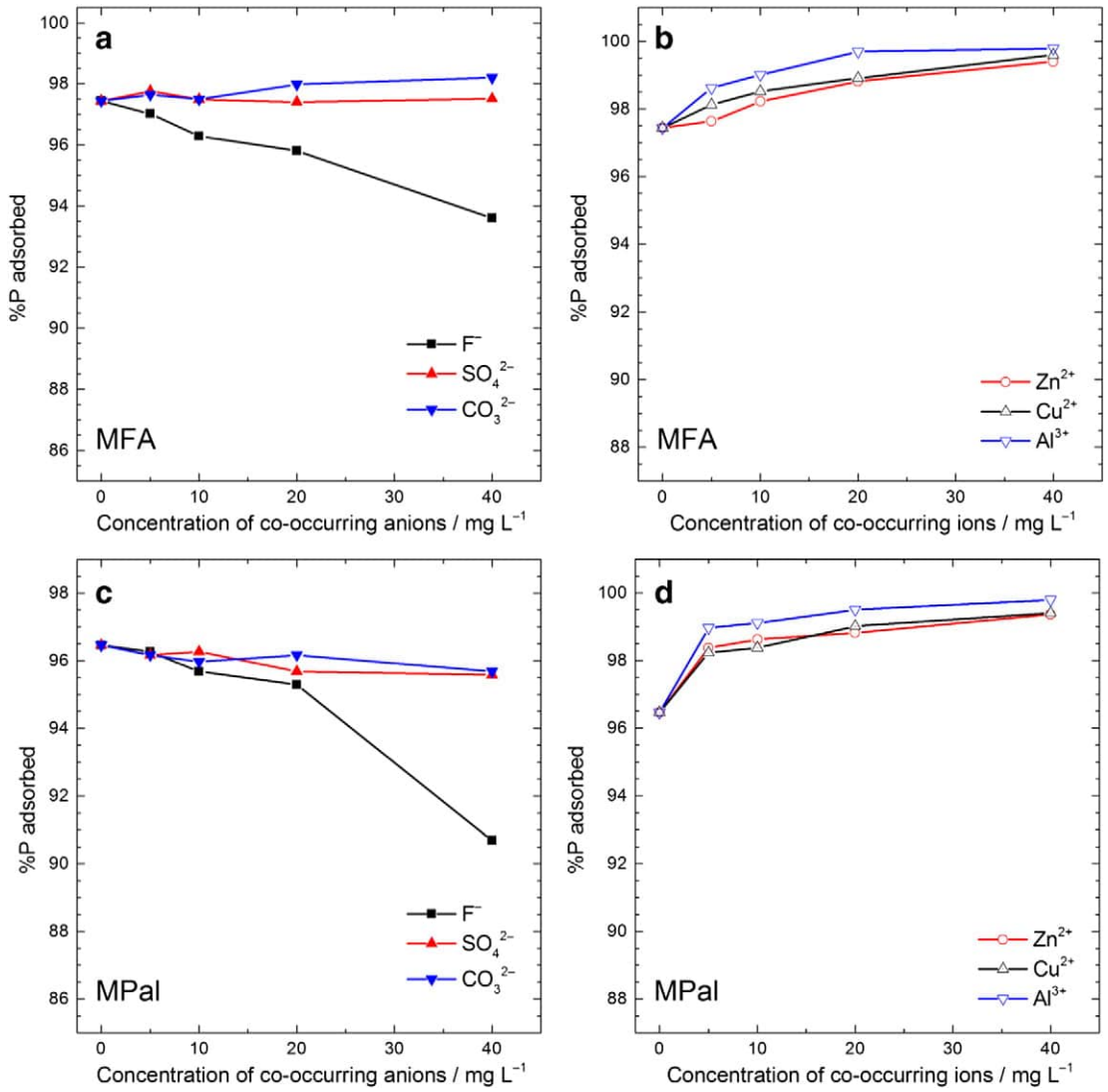

Fig. 6. Effect of co-occurring ions on phosphate adsorption.

phosphate adsorption over a variety of minerals (Karaca et al., 2004; Liao et al., 2006). Moreover, both adsorbents offer much faster phosphate uptake rate than the widely studied calcined palygorskite (Ye et al., 2006; Gan et al., 2009), Fe-based adsorbents (Liao et al., 2006; Wang et al., 2008) and clay minerals (Karaca et al., 2004; Gao et al., 2013), suggesting that both MFA and MPal are high efficient adsorbent alternatives for phosphate removal.

3.6. Adsorption isotherms

In order to determine the maximum adsorption capacities of MFA and MPal for phosphate, the adsorption isotherms were performed with varying phosphate concentrations at pH 7.5 ± 0.1. The adsorption capacity of phosphate increased with increasing temperature, indicating that phosphate adsorption by both adsorbents is an endothermic process. This was also observed for phosphate adsorption by other adsorbents (Banerjee et al., 2008). A nonlinear fitting of the adsorption isotherm data with either Eq. (3) or Eq. (4) has been conducted by using the OriginLab® OriginPro 9.0 software. The fitting results, as summarized in Table 3 and Fig. 8, elucidate that the Langmuir adsorption model ($R^2 > 0.99$), rather than the Freundlich model, can well describe the adsorption isotherm data, suggesting that phosphate adsorption was most likely occurring in a monolayer fashion.

The maximum adsorption capacities of phosphate at 298 K calculated by the Langmuir equation were 0.43 mmol (13.3 mg P) per g MFA and 0.34 mmol (10.5 mg P) per g MPal, respectively (Table 3). As given in Table 4, their maximum adsorption capacities are greater than those of adsorbents such as class F fly ash (6.6 mg P g^{-1}) (Agyei et al., 2002), natural (4 mg P g^{-1}) and acid-treated palygorskite (9 mg P g^{-1}) (Ye et al., 2006), and are comparable with those of Ca-rich blast furnace slag (10.5 mg P g^{-1}) (Johansson and Gustafsson, 2000) and calcined palygorskite (13.7 mg P g^{-1}) (Gan et al., 2009). To test the feasibility of both adsorbents to treat wastewater, an attempt of removing phosphate from municipal sewage with initial P concentration of 5.8 mg L^{-1} was made. The result (see Fig. S4) implies that all the measured parameters of the effluent were satisfactory with the limitation values specified by the *Discharge standard of pollutants for municipal wastewater treatment plant (GB 18918–2002)*, suggesting that both adsorbents can be used effectively in practice.

3.7. Thermodynamic analysis

Thermodynamic analysis is a useful tool for explanation of adsorption mechanism. Two thermodynamic parameters, i.e., the standard enthalpy change (ΔH^0) and free energy change (ΔG^0), can be obtained by calculation of adsorption isotherm data with Eqs. (5)–(7) (Table S2). For both adsorbents, ΔH^0 is positive, implying that phosphate adsorption by

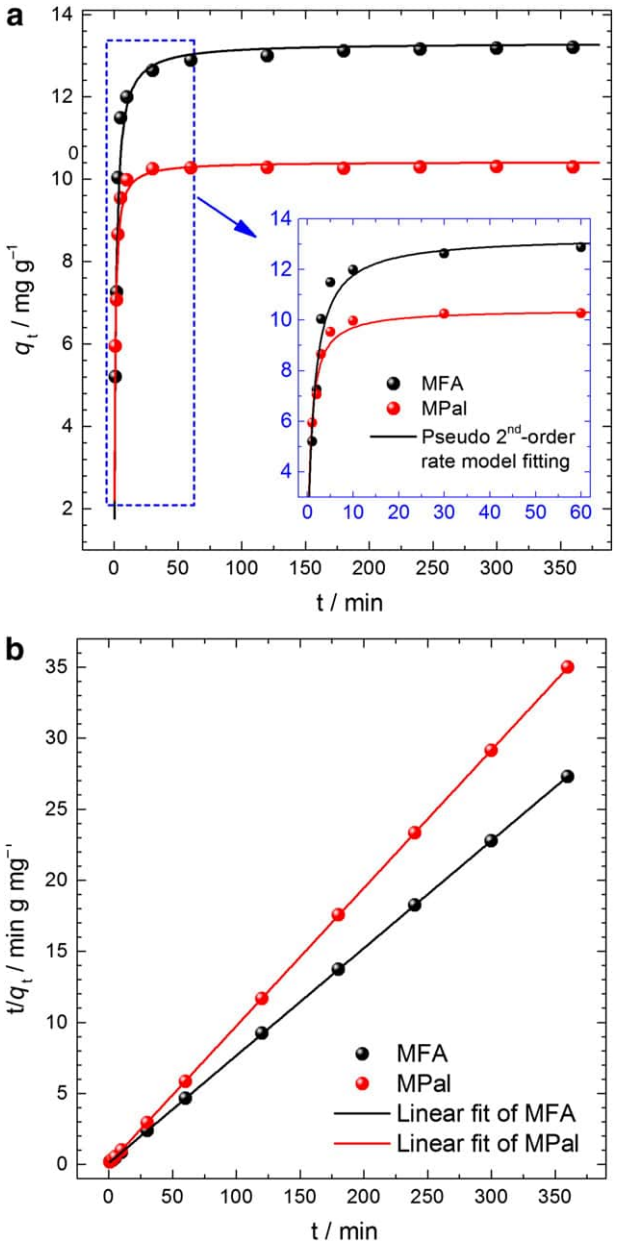

Fig. 7. Kinetic curves of phosphate adsorption on MFA and MPal: (a) $q_t \sim t$; (b) $t/q_t \sim t$, (pH 7.5 ± 0.1; $T = 298$ K).

both adsorbents is an endothermic process, in agreement with the above analysis. All ΔG^0 are negative, suggesting that phosphate adsorption at different temperatures are spontaneous. These analyses lead to a fact that a chemical adsorption mechanism may be involved in the adsorption process of phosphate by both MFA and MPal, which will be further discussed in the SCM section.

Table 2
Fitting parameters of pseudo 2nd-order rate model for adsorption of phosphate on MFA and MPal.

	Fitting parameters from pseudo 2nd-order rate model			
Adsorbent	k_2 (g mg^{-1}·min^{-1})	q_t (mg P g^{-1})	$q_{t=6\ h.}$ (mg P g^{-1})	R^2
MFA	0.056	13.32	13.19	0.999
MPal	0.195	10.31	10.28	0.999

Table 3
Fitting parameters of both the Langmuir and the Freundlich models for the adsorption of phosphate on MFA and MPal.

		Langmuir			Freundlich		
Adsorbent	T (K)	b (L mmol^{-1})	q_m (mmol P g^{-1})	R^2	K_F	n	R^2
MFA	283	35.36	0.38	0.993	5.52	2.82	0.974
	298	41.72	0.43	0.991	6.49	2.52	0.976
	313	56.73	0.47	0.997	8.20	2.27	0.987
MPal	283	36.48	0.30	0.990	5.47	4.49	0.953
	298	40.10	0.34	0.990	5.88	4.12	0.949
	313	50.53	0.37	0.991	5.52	2.81	0.954

3.8. Surface complexation modeling and adsorption mechanism

Many SCM models, including CCM (Goldberg and Sposito, 1984, 1985; Bleam et al., 1991; Nilsson et al., 1996; Gao and Mucci, 2001), basic stern model (BSM) (Gao and Mucci, 2001), diffuse double layer

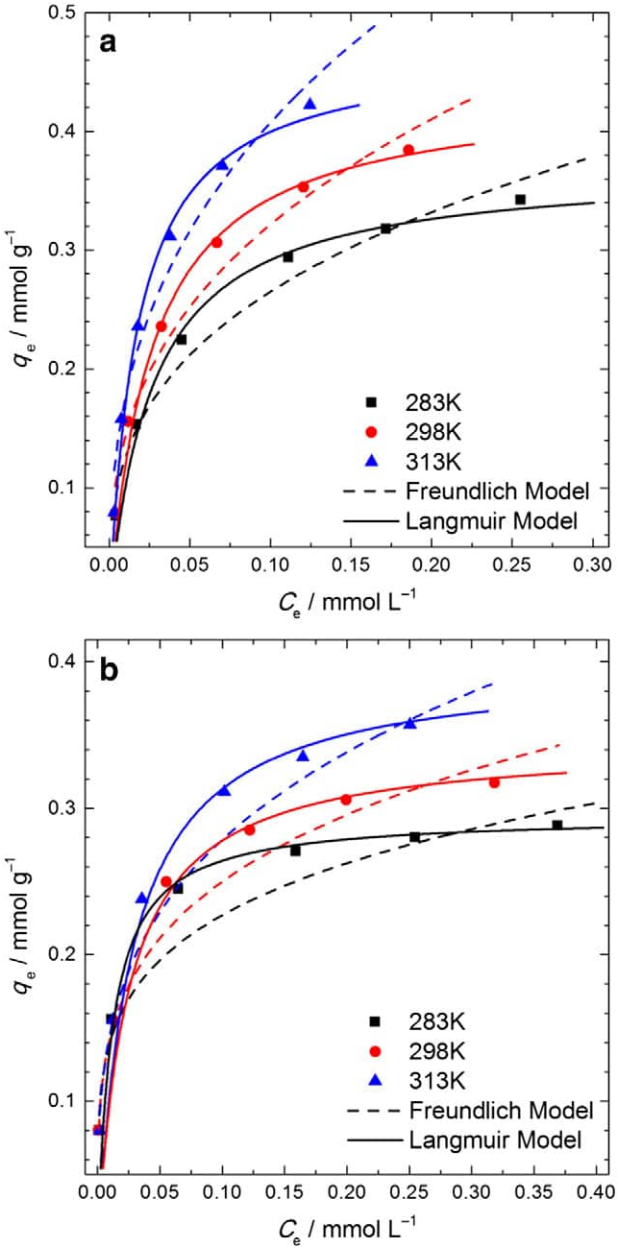

Fig. 8. Adsorption isotherms of phosphate on (a) MFA and (b) MPal.

Table 4
Reported maximum adsorption capacities of phosphate (mg P g^{-1}) on fly ashes and palygorskites at 298 K in literature.

Adsorbent	Capacity (mg P g^{-1})	Ref.
Class F fly ash	6.6	Agyei et al. (2002)
Ca-rich blast furnace slag	10.5	Johansson and Gustafsson (2000)
Natural palygorskite	4.0	Ye et al. (2006)
Calcined acid-treated palygorskite	9.0	Ye et al. (2006)
Calcined palygorskite	13.7	Gan et al. (2009)
MFA	13.3	This study
MPal	10.5	This study

model (DLM) (Butkus et al., 1998), triple layer model (TLM) (He et al., 1997; Gao and Mucci, 2001), and charge distribution model (CDM) (Rahnemaie et al., 2007), have been employed to well describe phosphate adsorption at various material/water interfaces over a range of solution conditions. Although based on different electric double layer models, all these models come to the same fact that phosphate were adsorbed mainly by ligand exchange to form inner-spheric complexes at the mineral/water interfaces (Goldberg and Sposito, 1984, 1985; Bleam et al., 1991; Nilsson et al., 1996; He et al., 1997; Gao and Mucci, 2001; Rahnemaie et al., 2007). On the basis of this fact, we used a generalized composite (GC) SCM without the electrostatic correction terms to simulate phosphate adsorption edge data (Fig. 9).

One general surface site (≡SOH) and two different surface sites (strong site, ≡SOH and weak site, ≡WOH) were proposed to best fit the experimental data for MFA and MPal, respectively (see Table S1). These constants were obtained from literature (see references in *SI*) with an assumption that ferrinol group (≡FeOH) and aluminol group (≡AlOH) (Vico and Acebal, 2006) are the main active binding sites for MFA and MPal, respectively. For MFA, the GC model is able to represent the experimental data well in pH range of 6–11, while in pH range of 3.5–6, the model underestimates the experimental data (Fig. 9a). This is possible due to the precipitation of a fraction of phosphate by dissolved Ca^{2+} from partly dissolution of gypsum in acidic pH range (Garverick, 1994). The model produces a close fit to the experimental data for MPal over the pH range of 4–12 (Fig. 9b), confirming the ability of GC model to describe phosphate adsorption in addition to fitting other radionuclides and metal ions adsorption (Davis et al., 1998, 2004).

Detailed ^{31}P solid-state NMR studies of phosphate adsorption on boehmite have indirectly confirmed that boehmite binds phosphate anion by displacing the surface hydroxyls (≡SOH) with phosphate anions and forming a monodentate complex (Bleam et al., 1991). Previous SCM modeling results also prefer a monodentate configuration to a bidentate binding mode between phosphate anion and metal oxides (Goldberg and Sposito, 1984, 1985; Bleam et al., 1991; Nilsson et al., 1996; He et al., 1997; Gao and Mucci, 2001), even though both bidentate and monodentate complexes were favorable in either CDM (Rahnemaie et al., 2007) or charge distribution-multisite surface complexation (CD-MUSIC) models (Antelo et al., 2010). Based on these precedents, we postulate that the phosphate anion is directly bound to the metal ions of these adsorbents, most likely in monodentate fashions as formulated in Eqs. (8)-(10). For the best fitting of experimental data with the GC model, two monodentate complexes, $\equiv SHPO_4^-$ and $\equiv SPO_4^{2-}$ are likely to form for both MFA and MPal in the current aqueous solution conditions.

3.9. Leaching characteristics of spent MFA and MPal

The leaching problem of spent adsorbents from industrial by-products (such as fly ash, red mud) is a crucial concern with regard to the post-adsorption disposal or reuse. As given in Fig. 10, the leaching test results indicate that both spent adsorbents have very limited leachable

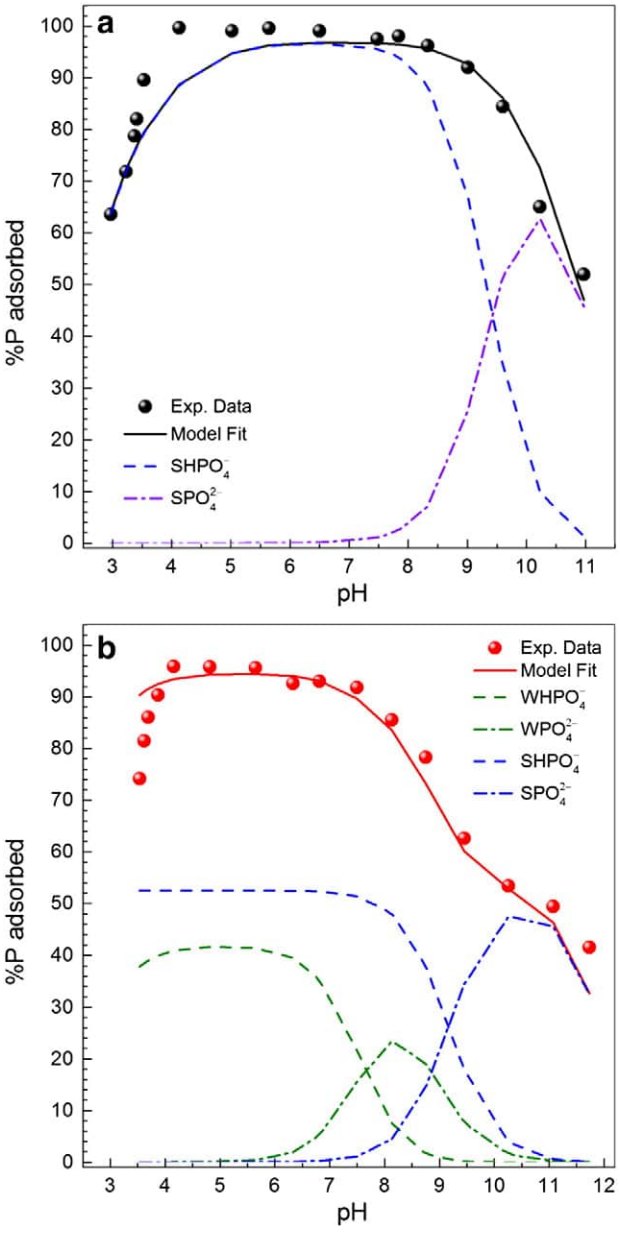

Fig. 9. Fitting results of phosphate adsorption edges with generalized composite (GC) modeling approach using the parameters given in Table S1. (a) MFA and (b) MPal.

toxic ions, e.g., chromium ions, copper ions, arsenic anions, zinc ions, and manganese ions. All of these toxin concentrations are far less than the maximum discharge concentrations (MDCs) as specified in *Discharge standard of pollutants for municipal wastewater treatment plant (GB 18918–2002)*. The reasons responsible for the low leaching toxic ions concentrations may include (i) the toxic heavy metal ions will react with phosphate to form less soluble products (Agyei et al., 2002; Bournonville et al., 2004), and (ii) the leaching of toxic elements is essentially low for class F fly ash (Grubb et al., 2000). The leaching tests of phosphate from the spent adsorbents were also performed to investigate the durability of phosphate retention. The results (Fig. 10) indicate that over 99% of phosphate was firmly retained by the adsorbents upon eluting treatment with excess water. Accordingly, both spent adsorbents can be safely disposed or further reused as starting materials for bricks or geopolymers (Lee and van Deventer, 2002). More recently, it is reported that surface activation with phosphate can enhance the ability of clay mineral to fix copper ion in aqueous solution (Siewe et

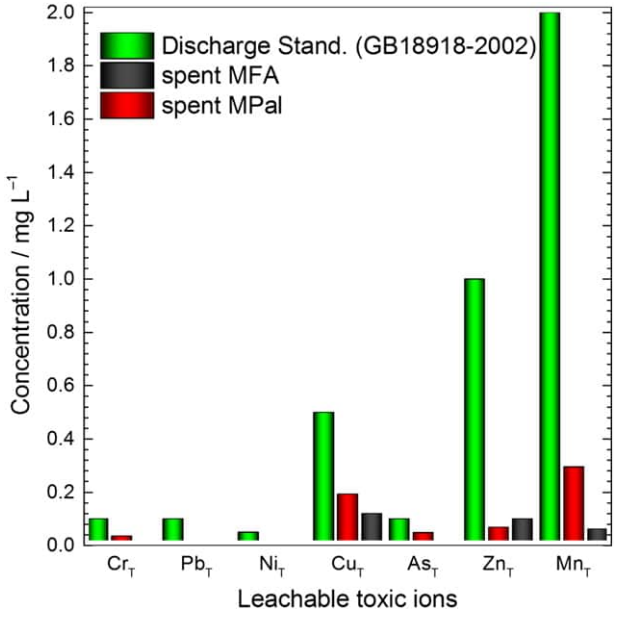

Fig. 10. Leachable toxic ions of spent MFA and MPal. (Note: the subscript T means total).

al., 2015), which implies that both spent MFA and MPal can be alternatively used in copper fixation in aqueous solution.

4. Conclusions

Phosphate adsorption by acid-modified fly ash (MFA) and palygorskite (MPal) have been studied in this work. The experimental results suggest that phosphate adsorption is enhanced by acid modification, and that phosphate adsorption is pH dependent for both MFA and MPal. That is, increasing pH in the acidic range led to increased phosphate adsorption, while further increasing pH in the alkaline range resulted in a decreased phosphate uptake. Thermodynamics and kinetics results indicate that phosphate adsorption on both adsorbents is spontaneous and the adsorption rates follow the pseudo second-order rate model. The Langmuir model is able to describe phosphate adsorption isotherm data and produces maximum adsorption capacities (298 K) of 13.3 mg P g^{-1} for MFA and 10.5 mg P g^{-1} for MPal, respectively, making them practicable in treating municipal sewage. This has been further verified by the leaching test results of spent adsorbents, showing that both spent adsorbents are safe enough for either disposal or reuse. The mechanisms of phosphate adsorption as modeled with the generalized composite (GC) surface complexation modeling approach indicate that phosphate was directly bound to the surface metal centers of MFA and MPal, likely forming two monodentate complexes, $\equiv SHPO_4^-$ and $\equiv SPO_4^{2-}$ by ligand exchange. The SCM modeling results also confirm the ability of GC model to predict phosphate adsorption behavior onto complex mineral mixtures. Leaching test results suggest that the spent adsorbents can be safely disposed or further reused.

Acknowledgments

The work was partially supported by NSFC Grant (51002080, 51310105009), open fund by Jiangsu Key Laboratory of Atmospheric Environment Monitoring and Pollution Control (KFK1505), PAPD program of Jiangsu Province and the JSNSF Grant (BK20141479). Mr. L. Yang is thankful for his experimental assistance. We thank two anonymous referees and Professor Vicente Rives for their helpful comments.

Appendix A. Supplementary data

Supplementary data to this article can be found online at http://dx.doi.org/10.1016/j.clay.2016.06.028.

References

Agyei, N.M., Strydom, C.A., Potgieter, J.H., 2000. An investigation of phosphate ion adsorption from aqueous solution by fly ash and slag. Cem. Concr. Res. 30, 823–826.
Agyei, N.M., Strydom, C.A., Potgieter, J.H., 2002. The removal of phosphate ions from aqueous solution by fly ash, slag, ordinary Portland cement and related blends. Cem. Concr. Res. 32, 1889–1897.
Antelo, J., Fiol, S., Perez, C., Marino, S., Arce, F., Gondar, D., Lopez, R., 2010. Analysis of phosphate adsorption onto ferrihydrite using the CD-MUSIC model. J. Colloid Interface Sci. 347, 112–119.
APHA, 1998. Standard Methods for the Examination of Water and Wastewater (Washington, DC, USA).
Atkins, P., De Paula, J., 2006. Physical Chemistry. eighth ed. W.H. Freeman and Company, New York, p. 212.
Banerjee, K., Amy, G.L., Prevost, M., Nour, S., Jekel, M., Gallagher, P.M., Blumenschein, C.D., 2008. Kinetic and thermodynamic aspects of adsorption of arsenic onto granular ferric hydroxide (GFH). Water Res. 42, 3371–3378.
Bergaya, F., Theng, B.K.G., Lagaly, G., 2006. Handbook of Clay Science. Elsevier, Amsterdam, The Netherlands, p. 261.
Bleam, W.F., Pfeffer, P.E., Goldberg, S., Taylor, R.W., Dudley, R., 1991. A P-31 solid-state nuclear-magnetic-resonance study of phosphate adsorption at the Boehmite aqueous-solution interface. Langmuir 7, 1702–1712.
Bournonville, B., Nzihou, A., Sharrock, P., Depelsenaire, G., 2004. Stabilisation of heavy metal containing dusts by reaction with phosphoric acid: study of the reactivity of fly ash. J. Hazard. Mater. 116, 65–74.
Butkus, M.A., Grasso, D., Schulthess, C.P., Wijnja, H., 1998. Surface complexation modeling of phosphate adsorption by water treatment residual. J. Environ. Qual. 27, 1055–1063.
Chen, J.G., Kong, H.N., Wu, D.Y., Chen, X.C., Zhang, D.L., Sun, Z.H., 2007. Phosphate immobilization from aqueous solution by fly ashes in relation to their composition. J. Hazard. Mater. 139, 293–300.
Correll, D.L., 1998. The role of phosphorus in the eutrophication of receiving waters: a review. J. Environ. Qual. 27, 261–266.
Das, J., Patra, B.S., Baliarsingh, N., Parida, K.M., 2006. Adsorption of phosphate by layered double hydroxides in aqueous solutions. Appl. Clay Sci. 32, 252–260.
Davis, J.A., Coston, J.A., Kent, D.B., Fuller, C.C., 1998. Application of the surface complexation concept to complex mineral assemblages. Environ. Sci. Technol. 32, 2820–2828.
Davis, J.A., Meece, D.E., Kohler, M., Curtis, G.P., 2004. Approaches to surface complexation modeling of uranium(VI) adsorption on aquifer sediments. Geochim. Cosmochim. Acta 68, 3621–3641.
Frost, R.L., Locos, O.B., Ruan, H., Kloprogge, J.T., 2001. Near-infrared and mid-infrared spectroscopic study of sepiolites and palygorskites. Vib. Spectrosc. 27, 1–13.
Gan, F.Q., Zhou, J.M., Wang, H.Y., Du, C.W., Chen, X.Q., 2009. Removal of phosphate from aqueous solution by thermally treated natural palygorskite. Water Res. 43, 2907–2915.
Gao, Y., Mucci, A., 2001. Acid base reactions, phosphate and arsenate complexation, and their competitive adsorption at the surface of goethite in 0.7 M NaCl solution. Geochim. Cosmochim. Acta 65, 2361–2378.
Gao, Y., Chen, N., Hu, W.W., Feng, C.P., Zhang, B.G., Ning, Q., Xu, B., 2013. Phosphate removal from aqueous solution by an effective clay composite material. J. Solut. Chem. 42, 691–704.
Garverick, L., 1994. Corrosion in the Petrochemical Industry. ASM International, Materials Park, OH, USA.
Gibbs, J.W., 1873. A method of geometrical representation of the thermodynamic properties of substances by means of surfaces. Trans. Connecticut Acad. Arts Sci. 382–404.
Goldberg, S., Sposito, G., 1984. A chemical-model of phosphate adsorption by soils 0.1. Reference oxide minerals. Soil Sci. Soc. Am. J. 48, 772–778.
Goldberg, S., Sposito, G., 1985. On the mechanism of specific phosphate-adsorption by hydroxylated mineral surfaces—a review. Commun. Soil Sci. Plant Anal. 16, 801–821.
Grubb, D.G., Guimaraes, M.S., Valencia, R., 2000. Phosphate immobilization using an acidic type F fly ash. J. Hazard. Mater. 76, 217–236.
Gustafsson, J.P., 2014. Visual MINTEQ version 3.1. http://www2.lwr.kth.se/English/OurSoftware/vminteq/index.htm (Stockholm, Sweden).
Haghseresht, F., Wang, S.B., Do, D.D., 2009. A novel lanthanum-modified bentonite, Phoslock, for phosphate removal from wastewaters. Appl. Clay Sci. 46, 369–375.
He, L.M., Zelazny, L.W., Baligar, V.C., Ritchey, K.D., Martens, D.C., 1997. Ionic strength effects on sulfate and phosphate adsorption on gamma-alumina and kaolinite: triple-layer model. Soil Sci. Soc. Am. J. 61, 784–793.
Ho, Y.S., McKay, G., 1998. Sorption of dye from aqueous solution by peat. Chem. Eng. J. 70, 115–124.
Huertas, F.J., Chou, L., Wollast, R., 1998. Mechanism of kaolinite dissolution at room temperature and pressure: part 1. Surface speciation. Geochim. Cosmochim. Acta 62, 417–431.
Johansson, L., Gustafsson, J.P., 2000. Phosphate removal using blast furnace slags and opoka-mechanisms. Water Res. 34, 259–265.
Karaca, S., Gurses, A., Ejder, M., Acikyildiz, M., 2004. Kinetic modeling of liquid-phase adsorption of phosphate on dolomite. J. Colloid Interface Sci. 277, 257–263.
Kasama, T., Watanabe, Y., Yamada, H., Murakami, T., 2004. Sorption of phosphates on Al-pillared smectites and mica at acidic to neutral pH. Appl. Clay Sci. 25, 167–177.

Lee, W.K.W., van Deventer, J.S.J., 2002. Effects of anions on the formation of aluminosilicate gel in geopolymers. Ind. Eng. Chem. Res. 41, 4550–4558.
Li, F.H., 2013. Layer-by-layer loading iron onto mesoporous silica surfaces: synthesis, characterization and application for as(V) removal. Microporous Mesoporous Mater. 171, 139–146.
Li, F.H., Zhai, J.P., Fu, X.R., Sheng, G.H., 2006a. Characterization of fly ashes from circulating fluidized bed combustion (CFBC) boilers cofiring coal and petroleum coke. Energy Fuel 20, 1411–1417.
Li, Y.Z., Liu, C.J., Luan, Z.K., Peng, X.J., Zhu, C.L., Chen, Z.Y., Zhang, Z.G., Fan, J.H., Jia, Z.P., 2006b. Phosphate removal from aqueous solutions using raw and activated red mud and fly ash. J. Hazard. Mater. 137, 374–383.
Liang, Z., He, X.J., Ni, J.R., 2010. Change of crystallinity and mineral composition of fly ash with mechanical and chemical activation for the improvement of phosphate uptake. Waste Manag. Res. 28, 901–907.
Liao, X.P., Ding, Y., Wang, B., Shi, B., 2006. Adsorption behavior of phosphate on metal-ions-loaded collagen fiber. Ind. Eng. Chem. Res. 45, 3896–3901.
Lu, S.G., Bai, S.Q., Zhu, L., Shan, H.D., 2009. Removal mechanism of phosphate from aqueous solution by fly ash. J. Hazard. Mater. 161, 95–101.
Mayer, B.K., Gerrity, D., Rittmann, B.E., Reisinger, D., Brandt-Williams, S., 2013. Innovative strategies to achieve low total phosphorus concentrations in high water flows. Crit. Rev. Environ. Sci. Technol. 43, 409–441.
Nilsson, N., Persson, P., Lovgren, L., Sjoberg, S., 1996. Competitive surface complexation of o-phthalate and phosphate on goethite (alpha-FeOOH) particles. Geochim. Cosmochim. Acta 60, 4385–4395.
Padmaja, P., Anilkumar, G.M., Mukundan, P., Aruldhas, G., Warrier, K.G.K., 2001. Characterisation of stoichiometric sol-gel mullite by Fourier transform infrared spectroscopy. Int. J. Inorg. Mater. 3, 693–698.
Pushpaletha, P., Lalithambika, M., 2011. Modified attapulgite: an efficient solid acid catalyst for acetylation of alcohols using acetic acid. Appl. Clay Sci. 51, 424–430.
Rahnemaie, R., Hiemstra, T., van Riemsdijk, W.H., 2007. Geometry, charge distribution, and surface speciation of phosphate on goethite. Langmuir 23, 3680–3689.
Siewe, J.M., Woumfo, E.D., Djomgoue, P., Njopwouo, D., 2015. Activation of clay surface sites of Bambouto's Andosol (Cameroon) with phosphate ions: application for copper fixation in aqueous solution. Appl. Clay Sci. 114, 31–39.
Tertre, E., Hofmann, A., Berger, G., 2008. Rare earth element sorption by basaltic rock: experimental data and modeling results using the "generalised composite approach". Geochim. Cosmochim. Acta 72, 1043–1056.
Ugurlu, A., Salman, B., 1998. Phosphorus removal by fly ash. Environ. Int. 24, 911–918.
Vico, L.I., Acebal, S.G., 2006. Some aspects about the adsorption of quinoline on fibrous silicates and Patagonian saponite. Appl. Clay Sci. 33, 142–148.
Wang, C.H., Auad, M.L., Marcovich, N.E., Nutt, S., 2008. Synthesis and characterization of organically modified attapulgite/polyurethane nanocomposites. J. Appl. Polym. Sci. 109, 2562–2570.
Wang, X.M., Li, W., Harrington, R., Liu, F., Parise, J.B., Feng, X.H., Sparks, D.L., 2013. Effect of ferrihydrite crystallite size on phosphate adsorption reactivity. Environ. Sci. Technol. 47, 10322–10331.
Wilkie, J.A., Hering, J.G., 1996. Adsorption of arsenic onto hydrous ferric oxide: effects of adsorbate/adsorbent ratios and co-occurring solutes. Colloid Surf. A Physicochem. Eng. Asp. 107, 97–110.
Xu, K., Deng, T., Liu, J.T., Peng, W.G., 2010. Study on the phosphate removal from aqueous solution using modified fly ash. Fuel 89, 3668–3674.
Xue, Y.J., Hou, H.B., Zhu, S.J., 2009. Characteristics and mechanisms of phosphate adsorption onto basic oxygen furnace slag. J. Hazard. Mater. 162, 973–980.
Yan, J.Y., Kirk, D.W., Jia, C.Q., Liu, X.N., 2007. Sorption of aqueous phosphorus onto bituminous and lignitous coal ashes. J. Hazard. Mater. 148, 395–401.
Ye, H.P., Chen, F.Z., Sheng, Y.Q., Sheng, G.Y., Fu, J.M., 2006. Adsorption of phosphate from aqueous solution onto modified palygorskites. Sep. Purif. Technol. 50, 283–290.
Zamparas, M., Gianni, A., Stathi, P., Deligiannakis, Y., Zacharias, I., 2012. Removal of phosphate from natural waters using innovative modified bentonites. Appl. Clay Sci. 62-63, 101–106.
Zhang, L.X., Jin, Q.Z., Shan, L., Liu, Y.F., Wang, X.G., Huang, J.H., 2010. $H_3PW_{12}O_{40}$ immobilized on silylated palygorskite and catalytic activity in esterification reactions. Appl. Clay Sci. 47, 229–234.
Zhang, H.R., Yang, H.J., Guo, H.J., Yang, J., Xiong, L., Huang, C., Chen, X.D., Ma, L.L., Chen, Y., 2014. Solvent-free selective epoxidation of soybean oil catalyzed by peroxophosphotungstate supported on palygorskite. Appl. Clay Sci. 90, 175–180.